AUT Journal of Civil Engineering

AUT J. Civil Eng., 6(1) (2022) 63-82
DOI: 10.22060/ajce.2022.20227.5764

Seismic Performance Assessment of a Masonry Arch Bridge Using Finite Element Method and Retrofitting by FRP

M. MollaJafari, F. Emami*, M. H. Hosseini

Department of Civil Engineering, Science and Research Branch, Islamic Azad University, Tehran, Iran.

ABSTRACT: Bridges are the most important and vulnerable crucial paths that damage them and result in significant financial disadvantages. A great part of the past technical and artistic documents are related to bridges and their construction techniques. Preservation of the historic bridges that are currently in use has particular importance. One of the historic bridges around Tehran that are located in the Firouzkuh fault zone, is Namroud Bridge. In the current study, the Namroud Stone Arc Bridge was investigated under strong ground motions to assess the weak points and to improve its behavior by retrofitting it. For this purpose, the finite element method was used for both modeling and nonlinear analyses under five near-field earthquake records. By recognizing the masonry bridge's weaknesses, FRP material was used to retrofit the bridge. The results reveal that although the studied bridge is vulnerable to earthquakes, it can maintain its stability. Further, the vertical acceleration component has an important effect on the vulnerability of the structure. Adding FRP sheets to the bridge deck was expressively effective whereas in other parts such as piers connection with the spandrel walls, leads to the spread of damage. Also in the location of the small openings, there is no possibility of the desired performance of FRP materials. Thus other methods such as planting rebar, injection, etc. should be used for these areas. Furthermore, it is impossible to use FRP material to achieve an economical and efficient method for retrofitting all bridge parts.

Review History:

Received: Jul. 02, 2021
Revised: Apr. 10, 2022
Accepted: Jun. 18, 2022
Available Online: Jun. 29, 2022

Keywords:

Masonry arch bridge
Seismic performance
Finite element method
Retrofit by FRP

1- Introduction

Bridges have always been one of the most important structures around us. A large part of the past technical and artistic evidence is related to bridges and bridge construction techniques. Erosion and damage factors of the bridge have been mentioned in different forms such as excessive loading, earthquake, groundwater leakage, surface water such as rainwater, and frost effect that usually result in cracking between blocks, mortar joints scour, weathering of stones and bricks, or the formation of hidden cavities inside the structure.

Cracking and slip phenomena, under mechanical forces, irrespective of their human (loading) or natural origin (earthquake), is known as damage [1]. In the past, masonry structures were constructed with trial and error without mathematical calculations, but using skill and experience, in recent years, numerical research methods have been used to predict the behavior of these structures [2].

In a study conducted on the Saint Martin masonry arch bridge, the bearing capacity of the arc and the need for its restoration were analyzed via the finite element model [3]. The seismic function of the Dutpınar Arch Bridge was investigated by the finite element method [4]. The studied bridge was analyzed dynamically by 3D finite element software ANSYS, then the responses, including stress, and principal strain, and displacements were assessed. A study was done on the seismic behavior of the Krakow masonry arch viaduct in Poland, under the foreshock and the main shock [5]. This structure was investigated under the components of the 2016 earthquake in Italy. To assess the effect of severe seismic motion on the Krakow Bridge, the concrete damage plasticity (CDP) model was defined, thus the possibility of damage evaluation was provided. Numerous studies have been done on the structural behavior of stone bridges in the past. Royles and Hendry [6] investigated the effect of embankment materials and spandrel walls on bridge resistance. Begimgil studied the weaknesses of the spandrel wall on a stone bridge with 1.25-meter spans [7]. Similar observations were obtained for the bridge test results under service operation loads by Boothby *et al.* [8]. Fanning and Boothby [9] analyzed the field test results of three existing stone arches bridges to determine the properties of appropriate materials. Brencich and Sabia [10] evaluated the behavior of the Tanaro Bridge in Italy. Milani and Lourenço [11] analyzed the three-dimensional nonlinear static behavior of two stone arch bridges by the finite element method. Sevim *et al.* [12] conducted a study on the linear seismic analysis of two historic bridges with modal

*Corresponding author's email: f-emami@srbiau.ac.ir

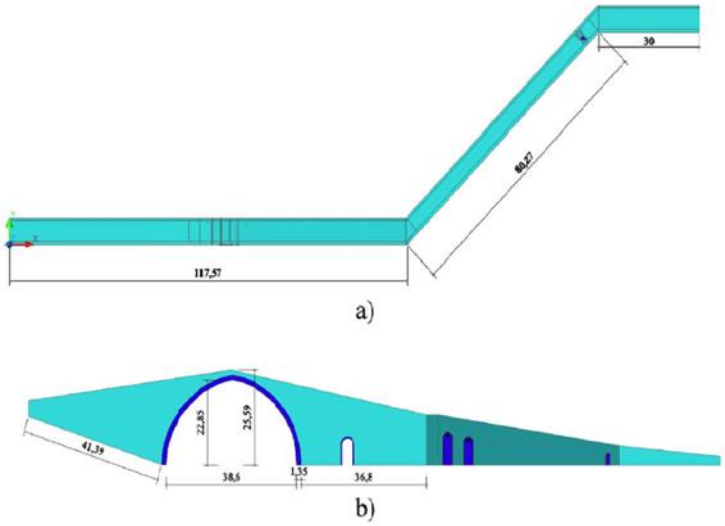

Fig. 1. Geometric dimension of Malabadi Bridge.

analysis. Sayın *et al.* [13] modeled a finite element model of the historic Uzunok Bridge and conducted linear and nonlinear analysis on the models. Pelà *et al.* [14] investigated the seismic evaluation of a three-arched stone bridge. Sayın [15] assessed the seismic response of the masonry bridge. To do this, he used artificial acceleration data in accordance with the seismic characteristics of the region. Nonlinear seismic performance of a 12th-century historical masonry bridge under different earthquake levels was conducted by Karaton *et al.* [16]. The seismic behavior of the Osmanli and Senyuva stone bridges was performed by a combination of FEM and DEM for getting closer to the real behavior of the bridge [17]. A simplified approach for seismic performance assessment of dry-joint masonry arch bridges was conducted by Demirel and Aldemir [18]. Concerning the necessity of investigating and condition of the masonry bridges in the earthquake, this study aims to investigate the Namroud stone bridge under earthquake loading using the finite element method, to assess the weaknesses of the bridge and achieve its behavior improvement by retrofitting.

2- Verification of modeling

For verification, an article entitled "Nonlinear seismic performance of a 12th-century historical masonry bridge under different earthquake levels" is examined that was conducted by Karaton *et al.* (2017) [16]. The Malabadi Bridge has a 38.6-meter span (Fig. 1) and it is the widest bridge in Anatolia-Turkey. To determine the parameters of the bridge materials, compressive strength tests, ultrasound testing, and the Schmitt hammer test was performed [19]. Homogeneous material properties are achieved for the macro modeling technique using the experimental results. A smeared crack model that includes tensile cracks and crushed compressive strength was selected for the behavior of the materials.

Finite element software ABAQUS was used for the verification in this study. To model the masonry components; the macro-modeling technique (homogeneous materials) was used in the present study by Karaton *et al.* [16]. In this method, the seams between materials such as stones, bricks, mortars, etc. are neglected and materials are considered homogeneous. After modeling the bridge in the software, the material specifications were given based on the results obtained from the tests of the reference paper [16], i.e., the density of materials was assumed to be 2250 kg/m^3. The nonlinear behavior of the materials was simulated using the concrete damaged plasticity (CDP) method. The parameters of this method were presumed based on the laboratory studies conducted by Jankowiak *et al.* [20]. The elastic and plastic specifications of the materials are shown in Table 1. The bridge damping is a proportion of the stiffness and mass and is equal to 5% of the vibrational mode on the bridge. Earthquake components produced as a synthetic method by considering the seismic characteristics of the region given in the reference article were applied to the bridge foundation (ground contact) and dynamic analysis was performed. To analyze such structures with nonlinear geometry or for structures with nonlinear materials, an explicit finite element analysis should be used. The synthetic acceleration and meshing model of the bridge is shown in Fig. 2.

After the analysis, the damaged regions appeared on the bridge as shown in Fig. 3. The first cracking zone in the bridge occurred at the upstream face of the bridge at 3.88 s. This zone is located on the right side of the main arc. There was no crack at the downstream face of the bridge in this step. After the first damage, another crack was created in the middle of the left side of the main arc, and this cracking region was caused by the main arc movement. Then, a new cracked area occurred in the middle of the right side of the main arc and the downstream face. After the fifth second, the main arc cracking mechanism occurred at the downstream and upstream faces of the bridge. It is observed that the locations of failures and cracks in the Karaton *et al.* model are coincident with

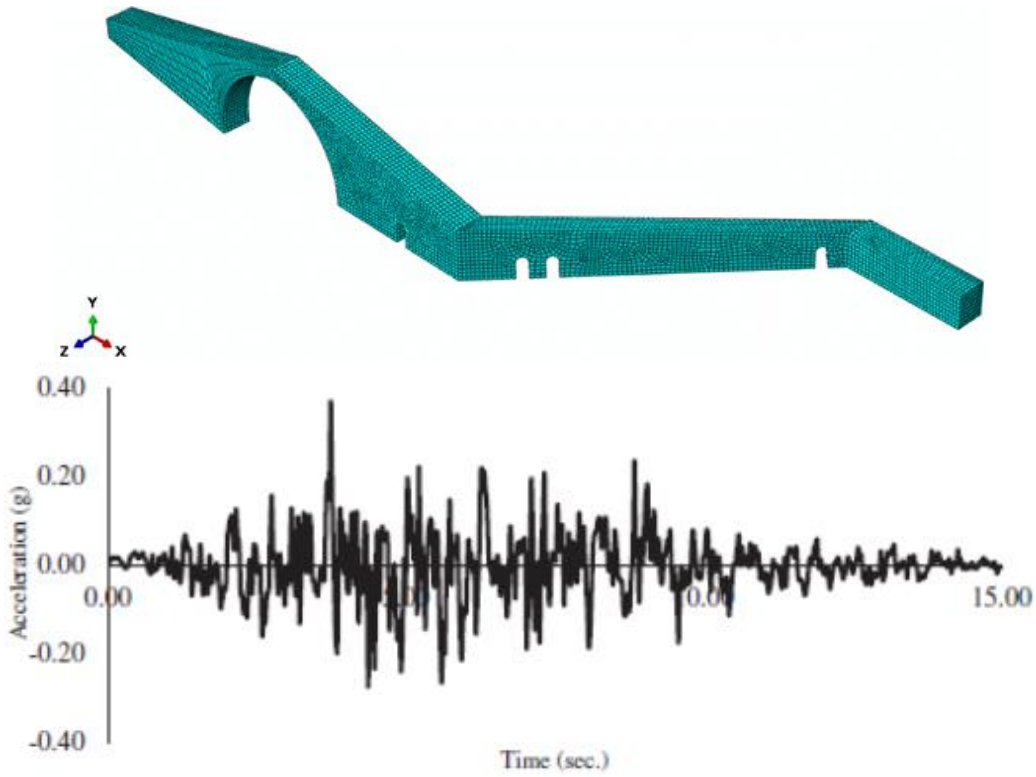

Fig. 2. The 3D meshed model of the bridge and applied synthetic acceleration data.

Table 1. Specification of the materials.

Material Properties		**The Parameters of the CDP model**	
E(Gpa)	19.7	β	˚38
υ	0.19	f	1.12
Compression Hardening		**Compression Damage**	
Stress [MPa]	**Strain [-]**	**Damage C [-]**	**Crushing Strain [-]**
15	0	0	0
20.19	0.0000747	0	0.0000747
30	0.0000988	0	0.0000988
40.30	0.000154	0	0.000154
50	0.000761	0	0.000761
40.23	0.00255	0.195402	0.00255
20.23	0.00567	0.596382	0.00567
5.25	0.01173	0.894865	0.01173
Tension Stiffening		**Tension Damage**	
Stress [MPa]	**Cracking Strain [-]**	**Damage T [-]**	**Cracking Strain [-]**
1.99	0	0	0
2.84	0.000033	0	0.000033
1.86	0.00016	0.406411	0.00016
0.86	0.000279	0.69638	0.000279
0.22	0.000684	0.920389	0.000684
0.056	0.00108	0.980093	0.00108

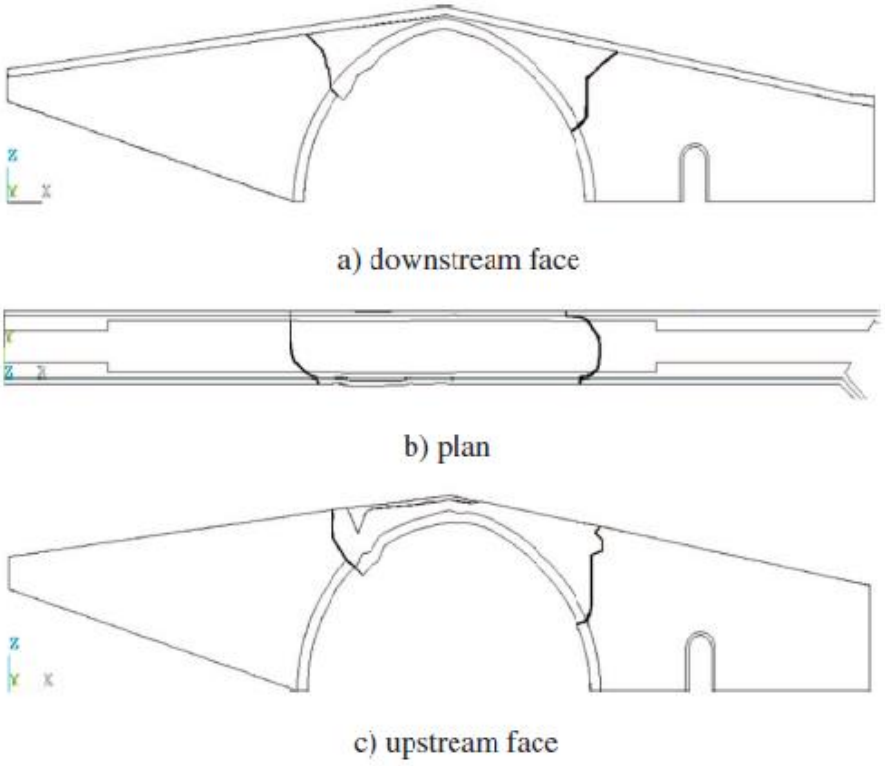

Fig. 3. Breakdown range.

the locations of maximum stress and maximum strain in the validation model. Since the exact location of the rupture has not been mentioned in the Karaton *et al.* model and only its range has been specified, it is impossible to compare the exact location of the cracks created in the two models, and thus, it is limited to the comparison of the range of failure. Vibrational modes are visible in both models in Figs. 4 and 5. Also, the periods of structural modes for both models after the modal analysis have been presented in Table 2.

As can be seen, there is an acceptable accommodation between the results of the karaton *et al.* and the verification model. The little difference between the structure period in the paper model and the verification model is due to the lack of dimensions and geometric details of the bridge, as well as the lack of access to the total specifications of the materials used in the paper model, and they are listed in the verification model as logical assumptions. As mentioned, by examining two models, it is observed that the crack regions in the karaton *et al.* model and verification model are in an acceptable match with the maximum stress and principal strain position. According to what was mentioned, the numerical model can be considered as the calibrated model and it can be used for other sensitivity analyses and parametric studies by considering the inherent similarity of the behavior of the samples with the aforementioned model.

3- Investigation and study of Namroud Masonary Bridge

In the current study, the Namroud Masonry Bridge is investigated under earthquake loadings, which is one of the bridges around Tehran and close to the Firouzkuh fault (Fig. 6). Field investigations show that the Namrud Bridge has been damaged in some parts. Therefore, it is necessary to evaluate the weaknesses of the bridge under earthquake loading and improve its behavior by retrofitting.

3- 1- Specification of materials

Regarding the material specification, it should be noted that due to the lack of field data from the mechanical and physical properties of the materials, all mechanical properties and the behavioral model of materials were presumed based on the laboratory studies conducted by Poole and Farmer [19] as well as Jankowiak *et al.* [20]. In fact, as a verification model, the density of materials was assumed to be 2250 kg/m^3 and the elastic and plastic specifications of the materials were utilized according to Table 1.

3- 2- Modeling and analysis

By field data from the studied bridge, its geometric dimensions and details were obtained. The 3D model was created by the finite element software ABAQUS. For modeling the structure, some details, such as the pier shoes and the small openings on the piers were neglected due to

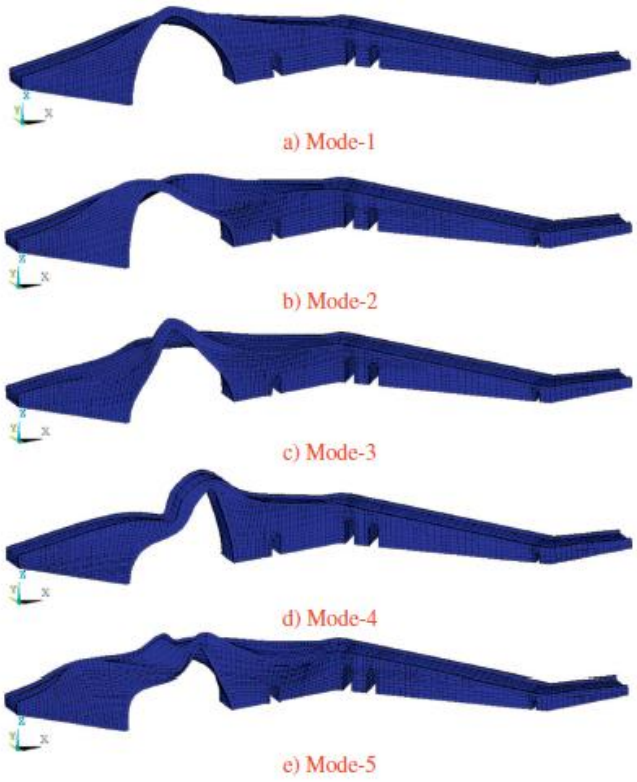

Fig. 4. Vibrational modes of the karaton et al. Model in Modal Analysis [16].

Table 2. Structural mode period in the verification model and paper model.

Model No.	Paper's model(sec)	Verification model(sec)
1	0.271	**0.212**
2	0.176	**0.124**
3	0.131	**0.086**
4	0.128	**0.077**
5	0.106	**0.068**
6	0.096	**0.066**
7	0.090	**0.063**
8	0.089	**0.056**
9	0.083	**0.053**
10	0.078	**0.053**

the prolongation of the analysis process but the other factors were considered and created according to the main structure and the obtained data from the field studies of the bridge. To model the structural components, a macro-modeling technique (homogeneous materials) was used, so that the seams or gaps between the elements and also the mortar were ignored and the structure was assumed to be homogeneous. To simulate the nonlinear behavior of materials, Concrete Damaged Plasticity (CDP) model was used. The parameters of this method were presumed based on the laboratory studies conducted by Jankowiak *et al.* [20]. Furthermore, for the studied bridge meshing, the dimensions of the mesh were selected 50 cm, and the number of created elements was 11843, and the elements were C3D8R i.e. 8-node linear brick, reduced integration, hourglass control element, but due to the presence of arch on Namroud masonry bridge, the meshes would not be cubic that may increase computing costs. The bridge damping was considered a ratio of stiffness and mass and equal to 5% of the vibrating mode on the bridge. The created model of Namroud Masonry Bridge was analyzed by the explicit dynamic method under earthquake records.

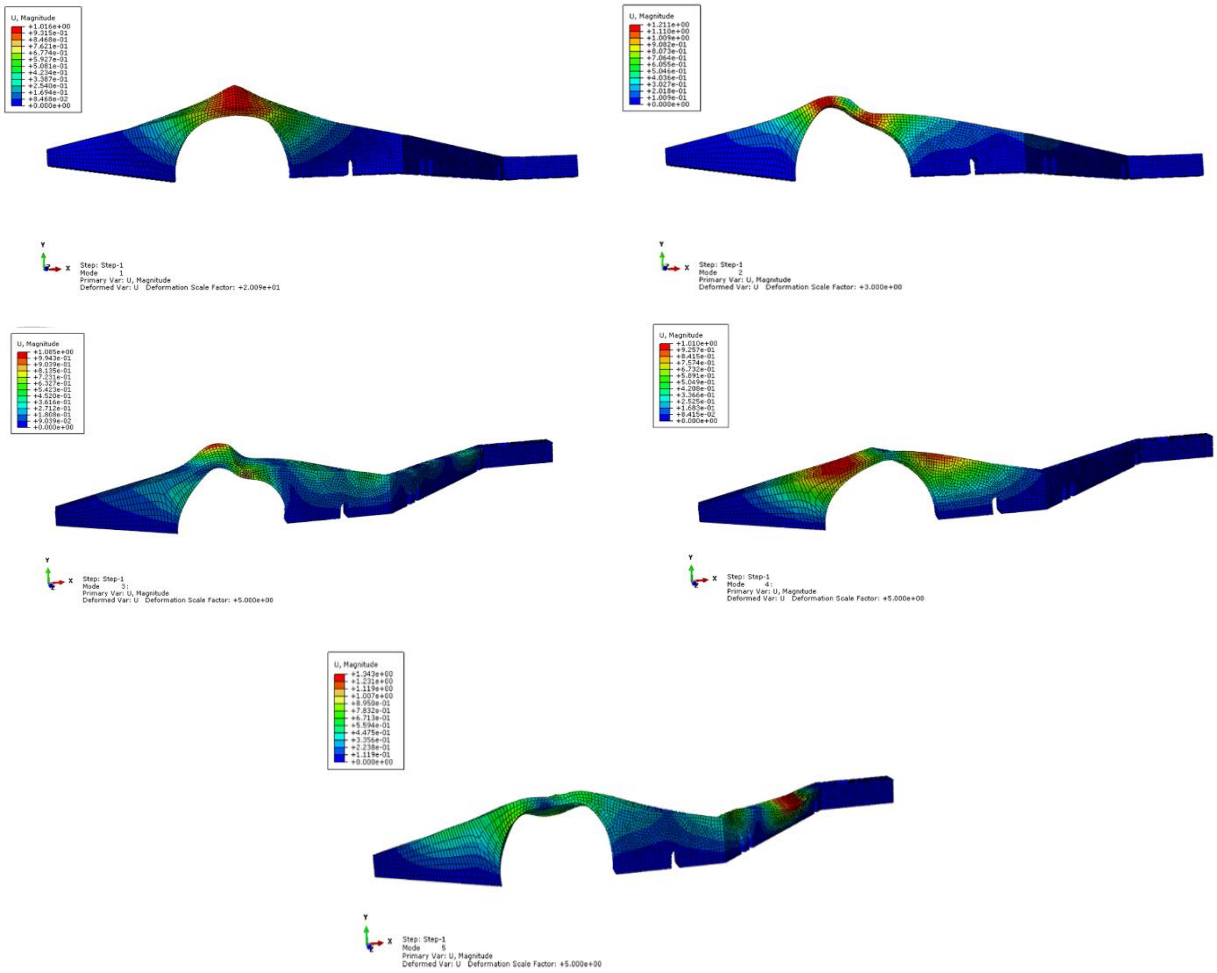

Fig. 5. Vibrational modes of the Verification Model.

3- 3- Specifications and modeling of FRP materials

Using FRP is one of the retrofitting methods applied in masonry arch bridges. Structural components retrofitted by FRP materials are beams, slabs, columns, walls, connections, and structures such as furnaces and chimneys, arches, domes, tunnels, silos, pipes, and trusses. FRP materials are also used to retrofit masonry, wood, steel, and cast iron structures. The used FRP materials have been assumed with the specifications of 200 and 20 Gpa modulus of elasticity in longitudinal and transverse directions of carbon fiber, respectively, the density of 1500 kg/m^3, shear modulus of 50 (xy & xz plane) and 5 Gpa (yz plane). Furthermore for modeling the FRP sheets, shell element S4R was used and connected to the bridge body by tie constraint.

3- 4- Earthquake records

In this analysis, the earthquake records of Tabas, Bam, Manjil, Zarand, and El Centro were used, and these records were applied to the bridge bases after scaling and obtaining the scale coefficient. Characteristics of records are shown in Table 3.

Earthquake records have been applied to bridge base in various conditions, these scenarios include:

Two simultaneous horizontal orthogonal components with DBE[1] hazard level

Three simultaneous horizontal and vertical components with DBE hazard level

The hazard level in this study was considered as type 1, based on which the design basic earthquake is an earthquake with a probability of exceedance10 % in 50 years and its return period is 475 years. To scale up the records, the standard design spectrum of Road and railway Bridges Seismic Resistant Design Code (No: 463) [21] was used for areas with high seismicity and on soil type II. Due to the presence of active faults near the area where the bridge has been located, the all of selected records are related to the near field and with a magnitude of more than 6 Richter. Also, the

1 Design-based Earthquake

Fig. 6. A view of the Namroud stone bridge and its dimension.

Table 3. Earthquake Specifications.

Row	Earthquake name	RSN	Year of occurrence	Station name	Magnitude earthquake	Distance from fault (km)
1	Manjil	1633	1990	Abhar	7.37	12.5
2	EL Centro	6	1940	El Centro	6.95	6.09
3	Tabas	143	1978	Tabas	7.35	1.79
4	Bam	4040	2003	Bam	6.6	0.05
5	Zarand	-	2005	Hotkan	6.4	7

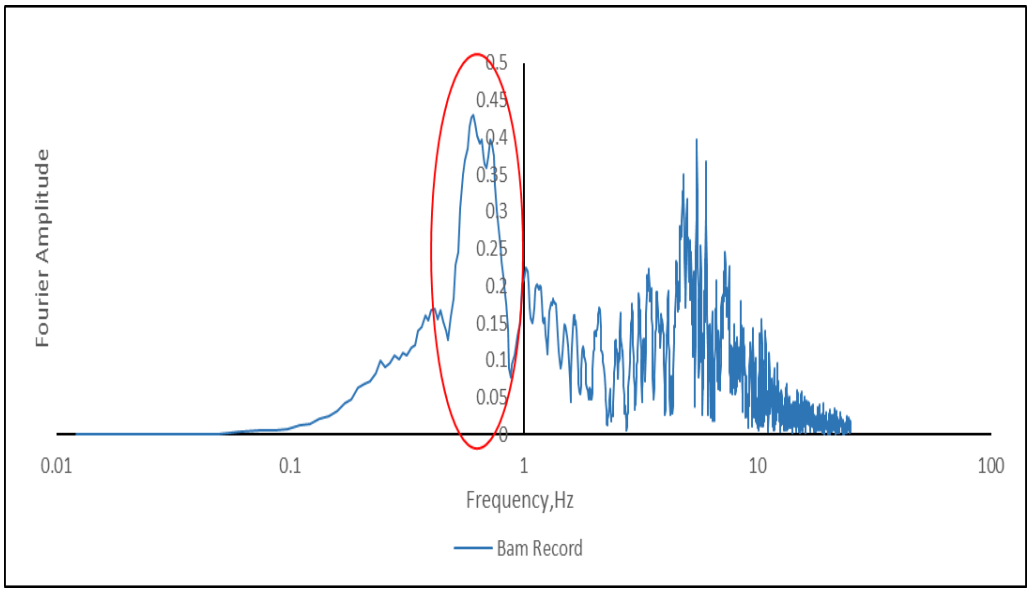

Fig. 7. Fourier amplitude-frequency curve for Bam record in two horizontal orthogonal components.

duration of the strong motion of the earthquake records is at least 10 seconds or 3 times the main period of the structure. To obtain the structure period, it is essential to conduct the modal analysis on the model, which was done and the structure period was obtained. For scaling the records, the response spectrum of horizontal components of each ground motion was determined and then the SRSS (the square root of the sum of the squares) of them was calculated. To do so, at first, the data of each record was entered into the Seismosignal software and the peak ground acceleration of each component was conveyed to 1, then the SRSS of the response spectrums of the horizontal components of each ground motion was calculated and the obtained SRSSs from all ground motions were averaged. Then, according to code 463, the obtained average response spectrum was compared with 1.4 times the standard spectrum of code 463 range for soil type II.

The average response spectrum must be such that in a range of $0.2T$ to $1.5T$ (T: the main period of the structure), i.e. 0.0064 and 0.048 seconds, in no case must be less than 1.4 times the standard spectrum. After the mentioned analogy, a coefficient was determined to observe the above tolerance, this obtained coefficient was considered as a scaling coefficient. In this research, the obtained coefficient is equal to 0.541.

4- Analyzing the results

The results of the nonlinear time history analyses done on the models in the form of the principal maximum plastic strain contours that indicate the cracking of the material and also the longitudinal displacement of the bridge are presented in this section.

4- 1- Two simultaneous horizontal orthogonal components with DBE hazard level in unreinforced states

As seen in Figs. 7 to 16, in all cases, damages to the bridge are very limited and insignificant. The reason for the limited vulnerability of the bridge against earthquakes with Design Base Earthquake (DBE) hazard level can be found at the very high structure frequency due to the considerable stiffness caused by the bridge's thick seams, so that even due to the relative weight of the bridges, which causes the structure not to enter the nonlinear region. In other words, the frequency of the first mode of the bridge is 31 Hz (T_1=0.032 sec) thus the dominant frequency of earthquake records according to Figs. 7, 9, 11, 13, and 15 has a relatively large distance with the frequency of the first mode of the structure.

4- 2- Three simultaneous horizontal and vertical orthogonal components with DBE hazard level in unreinforced states

As shown in Figs. 17 to 21, the severity of the damage is greater than the case in which the records were applied to the bridge in the two orthogonal components state. The reason for such a rise in vulnerability is the existence of vertical acceleration components in the bridge, which, in addition to creating substantial tensile stresses in the bridge piers, lead to a reduction in the shear capacity of the piers against the horizontal orthogonal components. Also the created tensile stresses due to the vertical component caused cracks in the pier, the spandrel wall, the abutment, and the bridge deck. These cracks in the structure were caused by the Manjil, Tabas, and El Centro earthquakes and in the case of the Bam and Zarand earthquakes, no tensile damage was observed.

4- 3- The three simultaneous horizontal and vertical orthogonal components with DBE hazard levels in reinforced states

Among the various options to retrofit this bridge, such as shotcrete, adding coils, steel jackets, grout injection between rocky components, etc., adding FRP sheets to the external

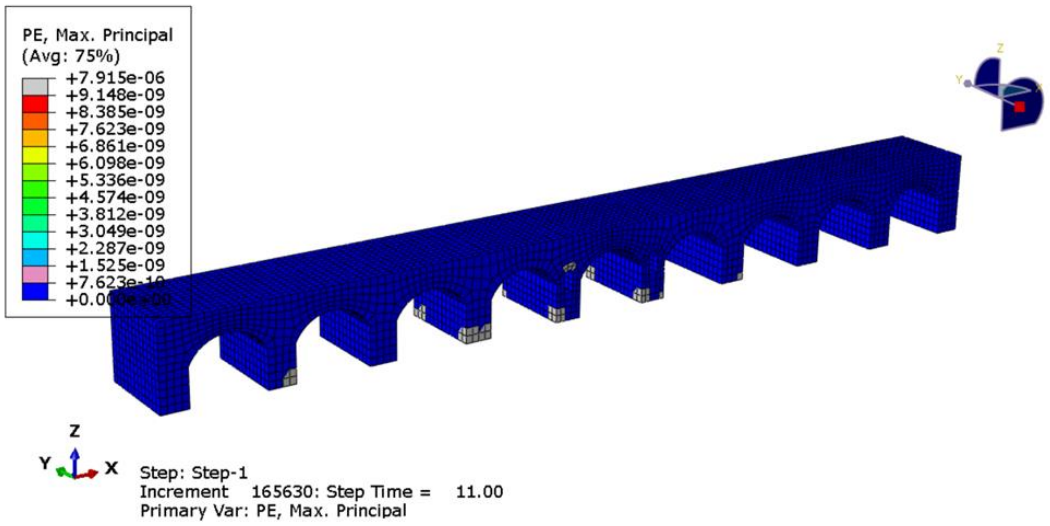

Fig. 8 .Maximum principal plastic strain contour of Bam record in the case of two simultaneous horizontal orthogonal components.

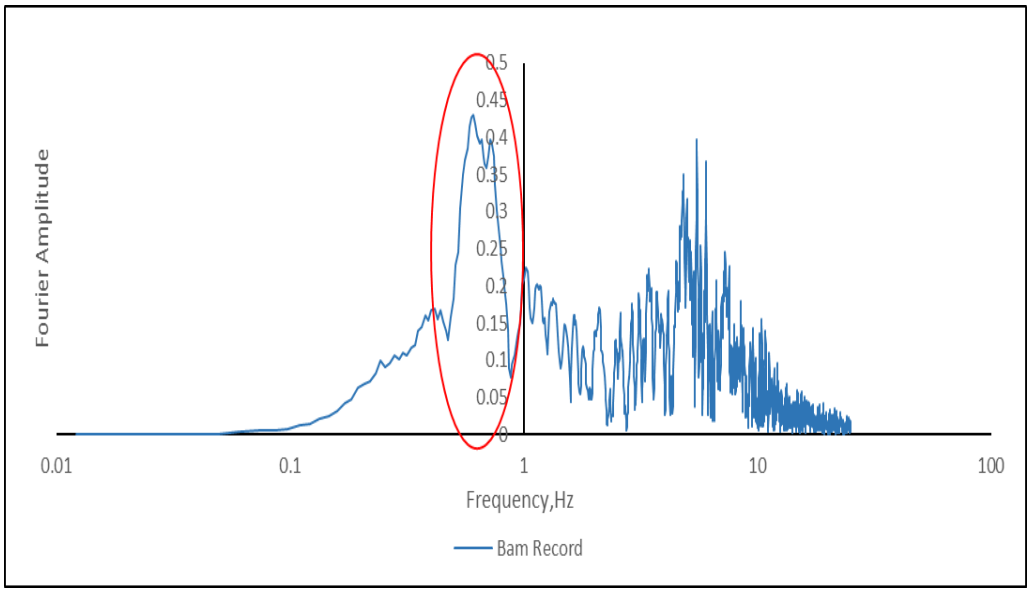

Fig. 9. Fourier amplitude-frequency curve for the El Centro record in the case of two horizontal orthogonal components.

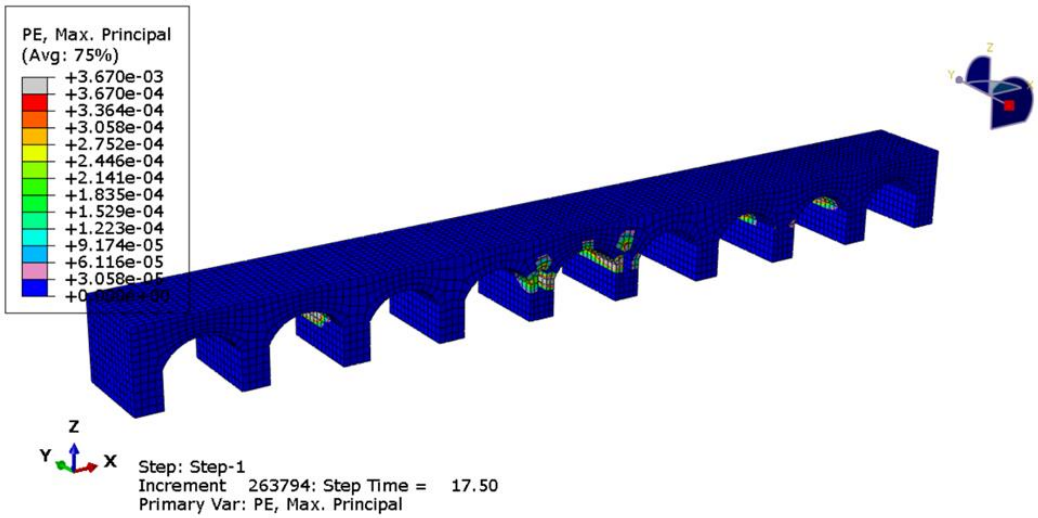

Fig. 10. Maximum principal plastic strain contour of El Centro record in the case of two simultaneous horizontal orthogonal components.

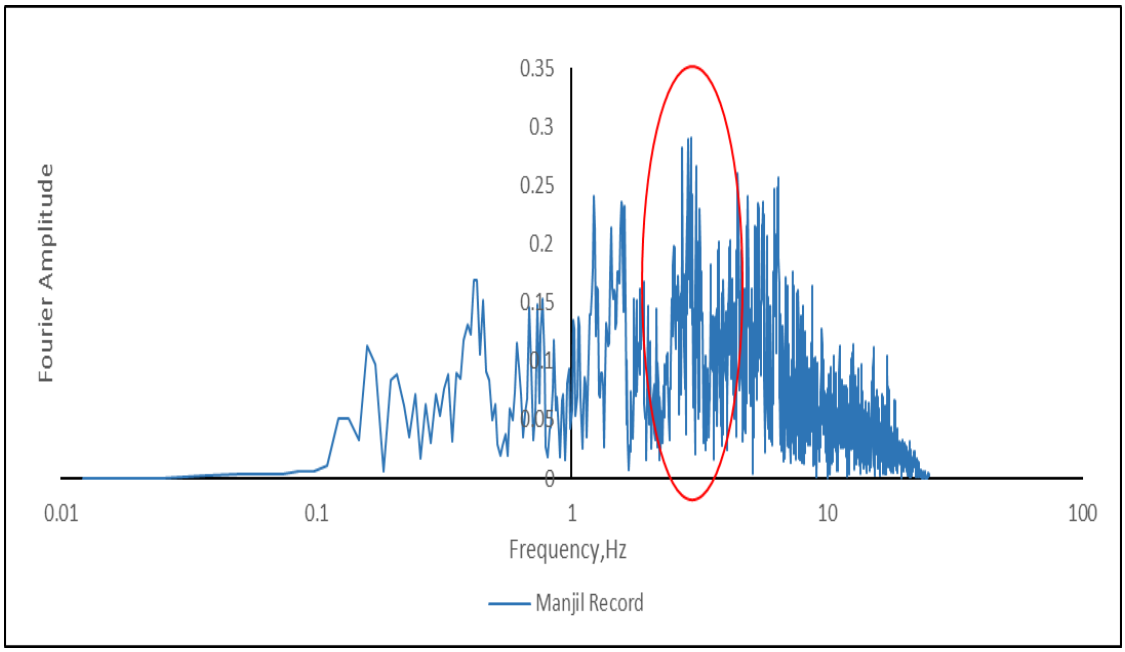

Fig. 11. Fourier amplitude-frequency curve for Manjil record in the case of two horizontal orthogonal components mode.

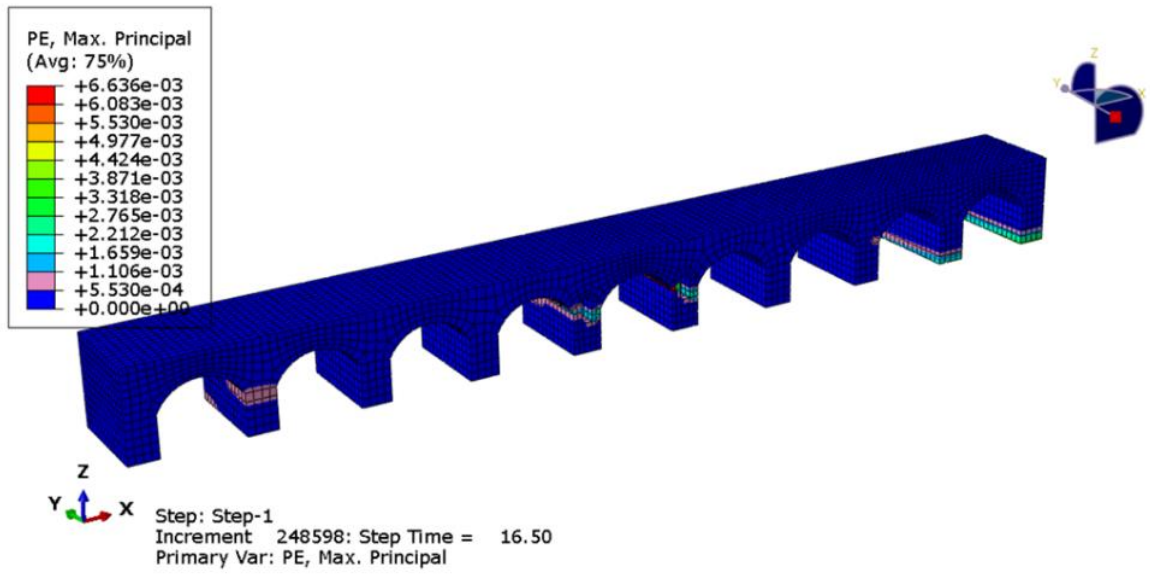

Fig. 12. Maximum principal plastic strain contour of Manjil record in the case of two simultaneous horizontal orthogonal components.

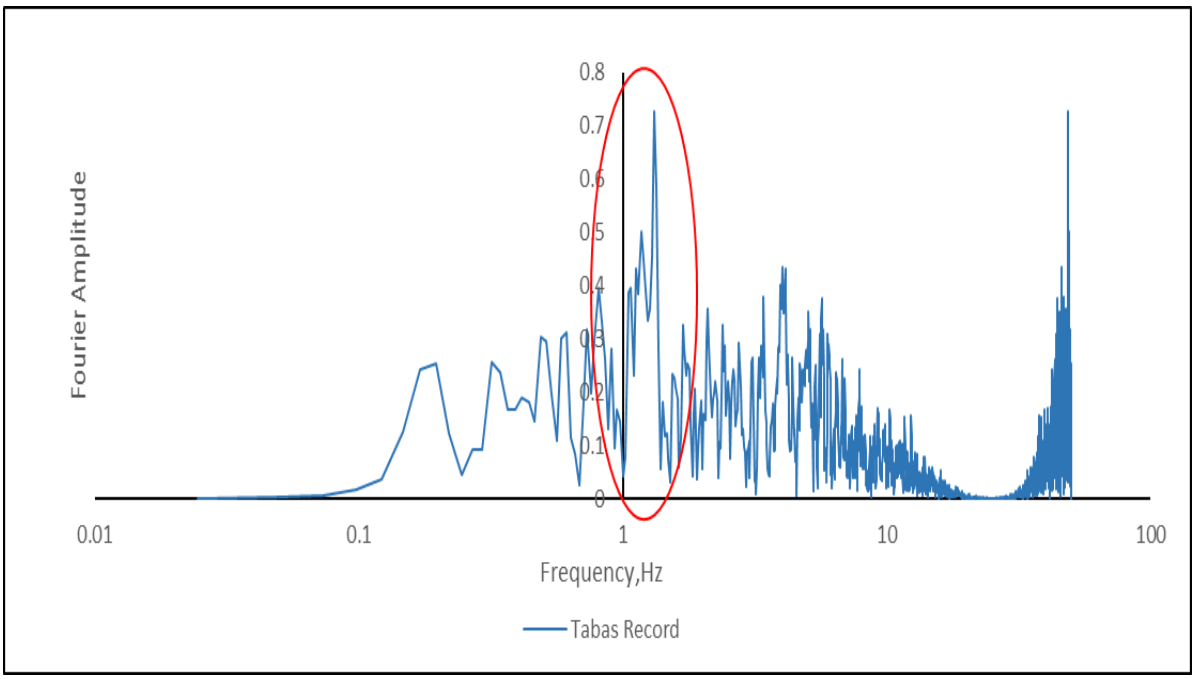

Fig. 13. Fourier amplitude-frequency curve for Tabas record in the case of two horizontal orthogonal components.

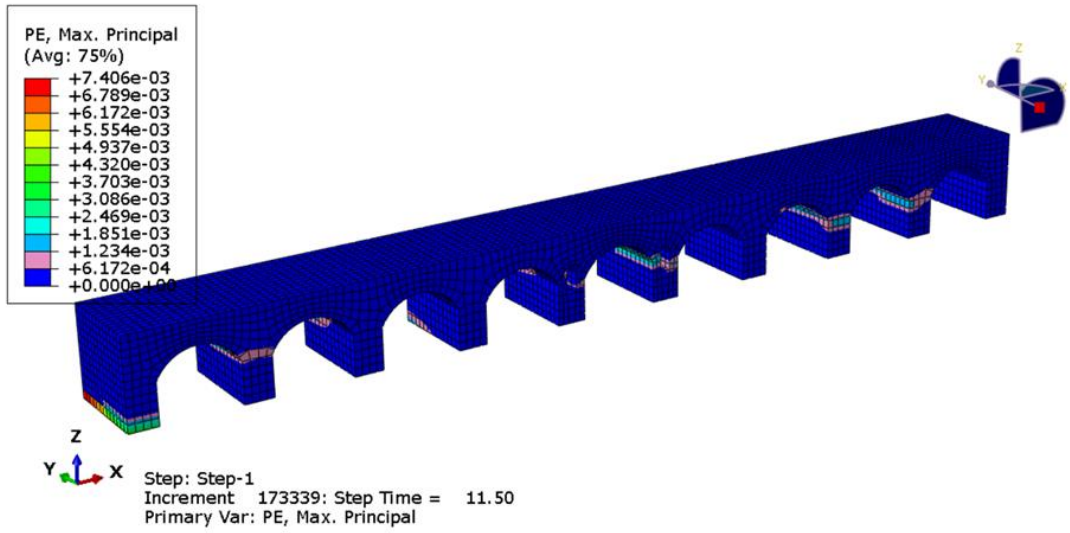

Fig. 14. Maximum principal plastic strain contour of Tabas record in the case of two simultaneous horizontal orthogonal components.

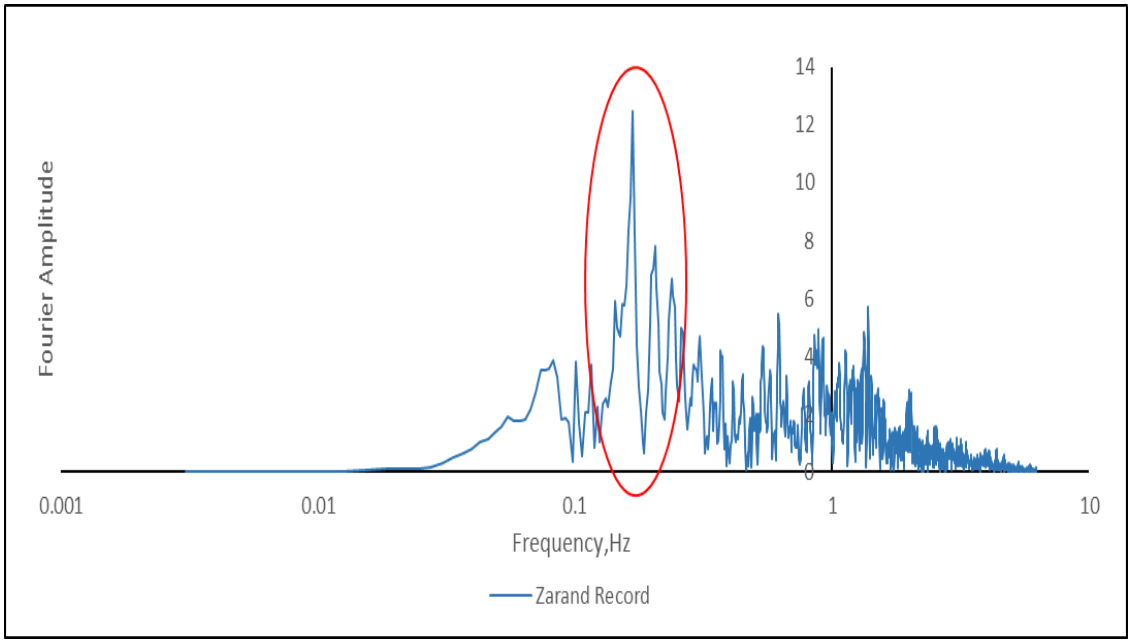

Fig. 15. Fourier amplitude-frequency curve for the Zarand record in the case of two horizontal orthogonal components.

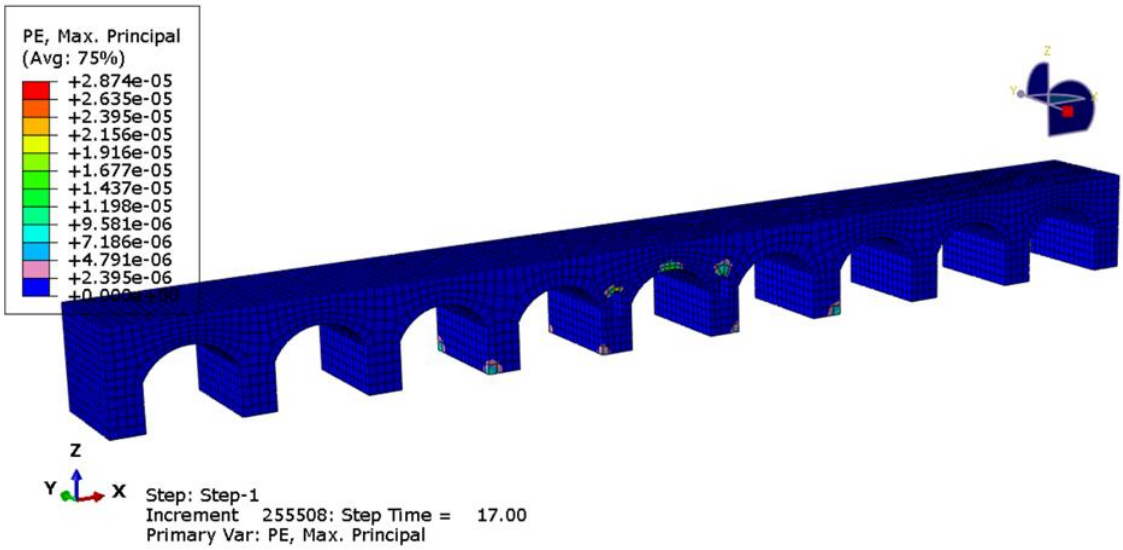

Fig. 16. Maximum principal plastic strain contour of Zarand record in the case of two simultaneous horizontal orthogonal components.

sides of the bridge was considered. In the current study, the FRP layer with a 200 GPa elasticity modulus, a density of 1500 kg/m^{3,} and a thickness of 2 and 3 mm was placed on the external surfaces of the models. It should be noted that the stresses at different times of the earthquake on this layer were investigated in order not to exceed the lower level of tensile stresses in comparison with the tear resistance of FRP, which is equal to 4950Mpa. In the following, the principal maximum tensile contours and tensile cracking contours are presented in the reinforced state.

4- 3- 1- Investigating the results of analyses in the case of the three-component mode under the Manjil earthquake in the reinforced state

According to the results of the analysis obtained in section 4.2, the bridge under the Manjil earthquake has happened tensile cracks significantly (90% reduction in capacity) in three areas, including the lower parts of the abutments and also the middle of the bridge deck. Therefore, to strengthen these areas, FRP with carbon fibers according to the specifications given in section 4.3 has been used. The width of the FRP layers used for the deck is equal to 2 meters, in length equal to the width of the deck, and to strengthen the piers, the FRP strips to a height of 1.4 meters from the pier were used in a wrapped state with a thickness of 2 mm. Regarding the selected thickness, it is necessary to explain that at first the thickness of the FRP was assumed to be 0.15 mm, and step by step and after successive analyzes, the thickness was added to achieve the desired result. In the third step, the thickness of FRP was selected as 1 mm, which was not enough to strengthen the piers. Then a thickness of 2 mm was selected, which was more suitable for both the deck and the piers. The result of the analysis is presented in Fig. 22.

In the following, to eliminate the damages in other piers, the reinforcing regions are expanded and the cracked parts were retrofitted by FRP with the indicated specifications and dimensions, the results of which are shown in Fig. 23.

The results obtained in this section also indicate that the breakdown and cracks in the bridge are still progressing, because by retrofitting the damaged piers in the previous stage, though significant improvement is observed in the performance of the mentioned piers, the damage has been transferred to other areas which have not been retrofitted. This incident shows that to retrofit the bridge, other retrofitting methods have to be used, such as planting rebar and injection, and so on. The final result of the analysis of the bridge retrofitted by FRP is presented in Fig. 24.

According to the above figures, the function of FRP is suitable for the piers without opening and can be a suitable option for retrofitting these types of piers. The result of the retrofitting of this structure under the Manjil earthquake is that FRP is a good option to fix the spandrel wall and deck,

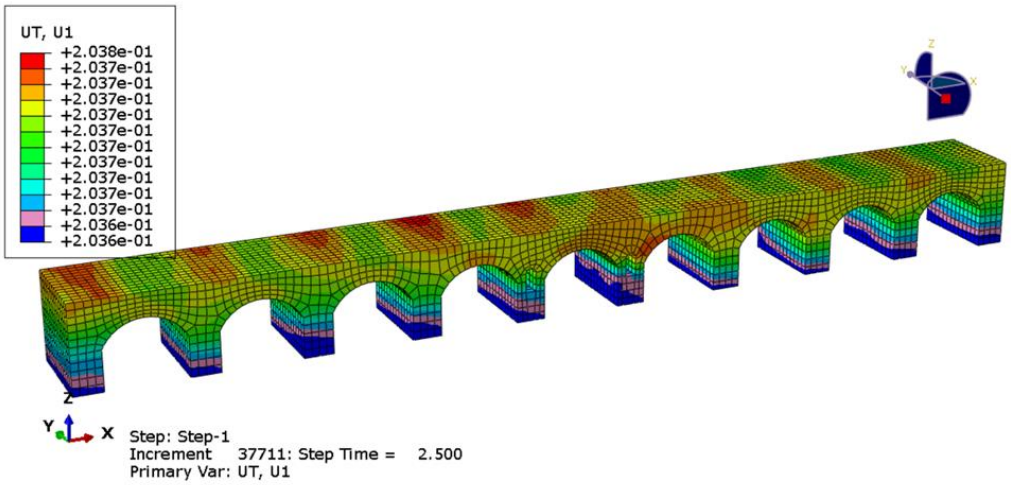

Fig. 17. The maximum longitudinal displacement contour of the bridge under the Bam earthquake in the three horizontal and vertical components.

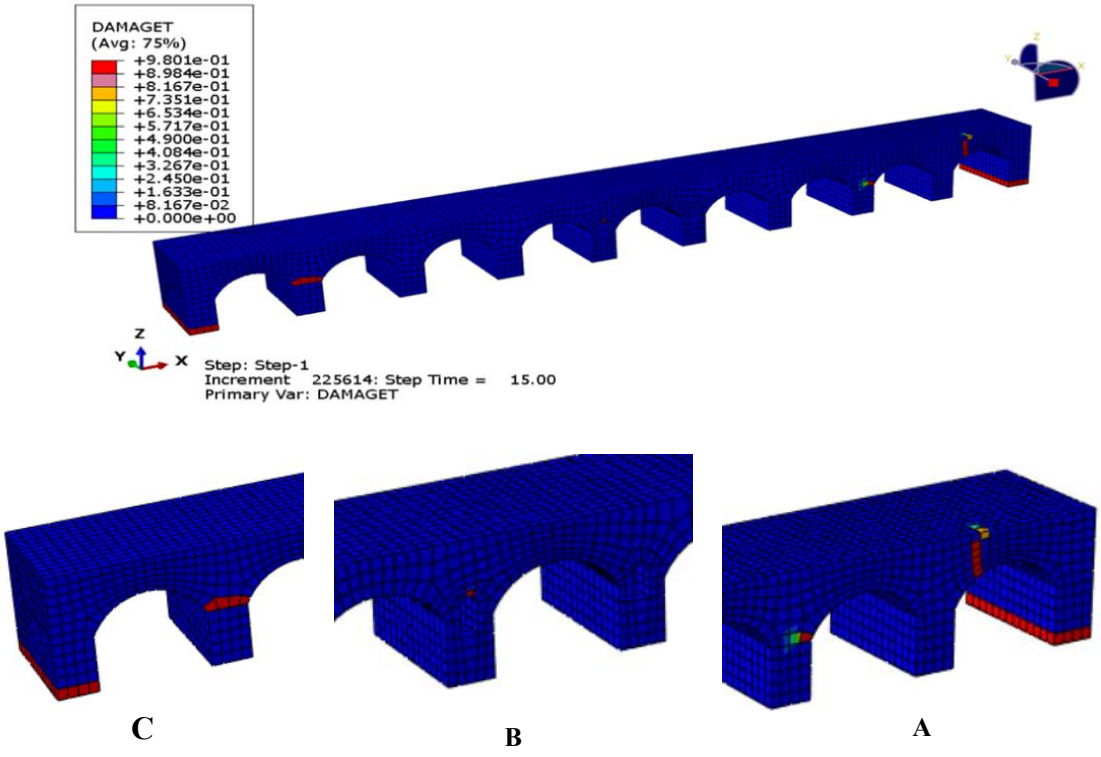

Fig. 18. The place of structural cracking of the bridge under the El Centro earthquake in the case of three horizontal and vertical components.

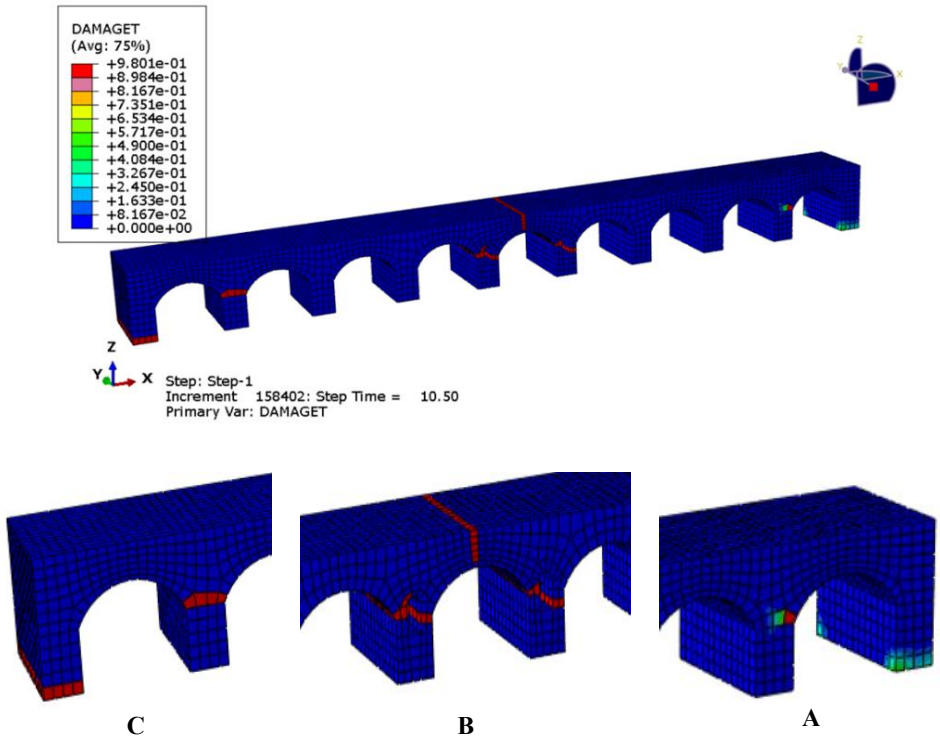

Fig. 19. The location of structural cracking of the bridge under the Manjil earthquake in the case of three horizontal and vertical components.

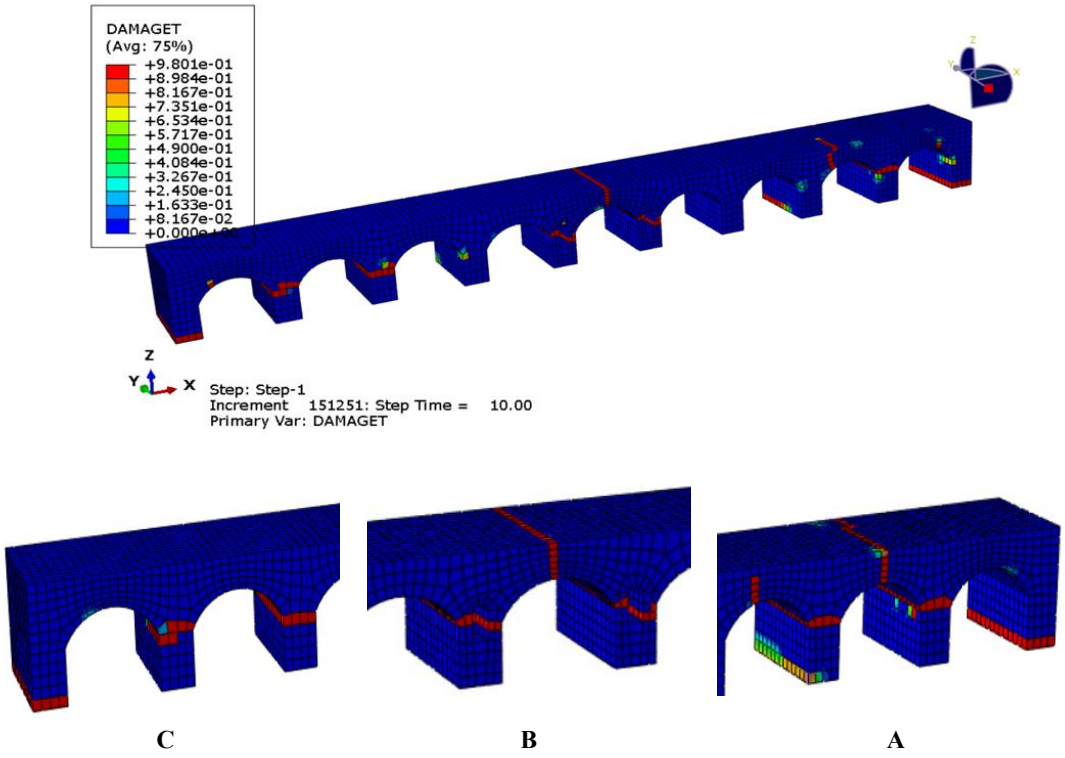

Fig. 20.The location of structural cracking of the bridge during the Tabas earthquake in the state of three horizontal and vertical components.

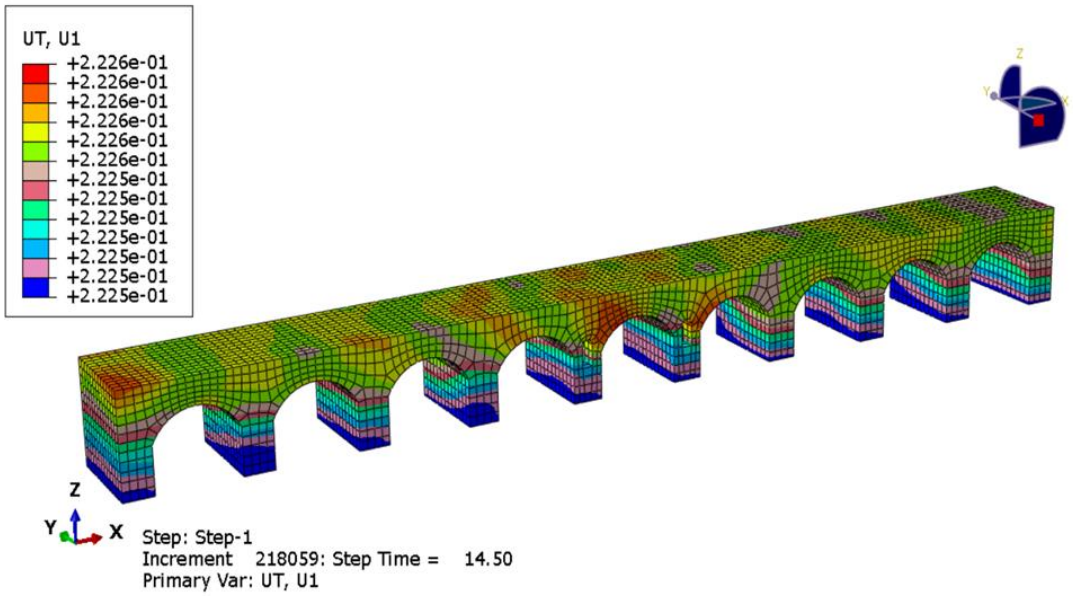

Fig. 21. The maximum longitudinal displacement contour of the bridge under the Zarand earthquake in the case of three horizontal and vertical components.

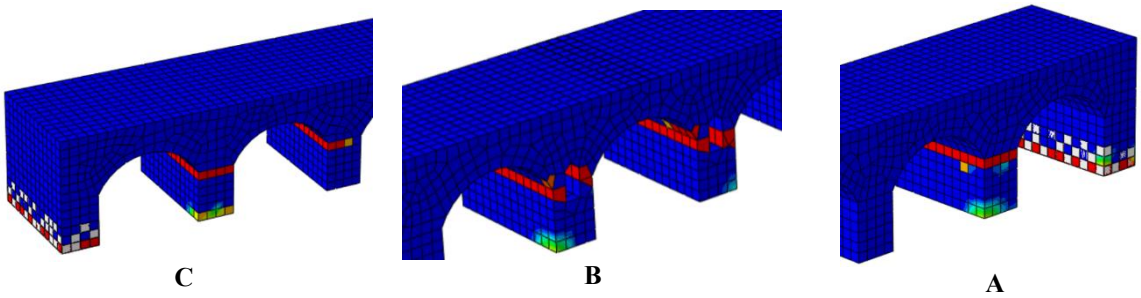

Fig. 22. The structural damage contour under the Manjil earthquake in the first step of retrofitting.

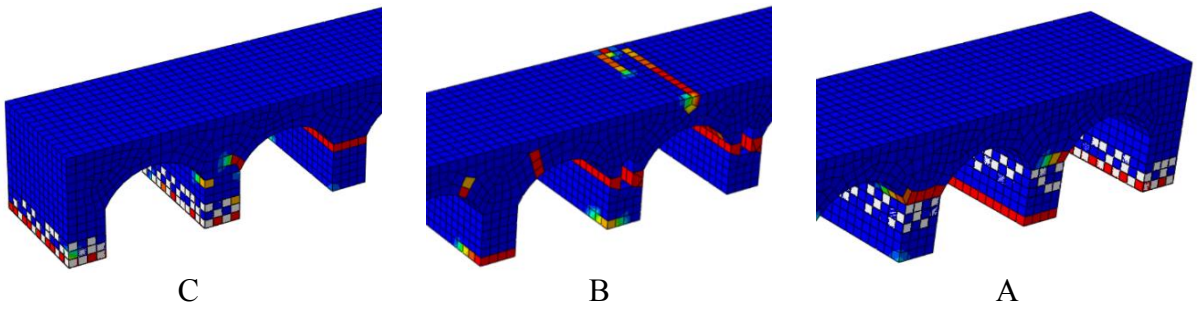

Fig. 23. The structural damage contour under the Manjil earthquake in the second step of retrofitting.

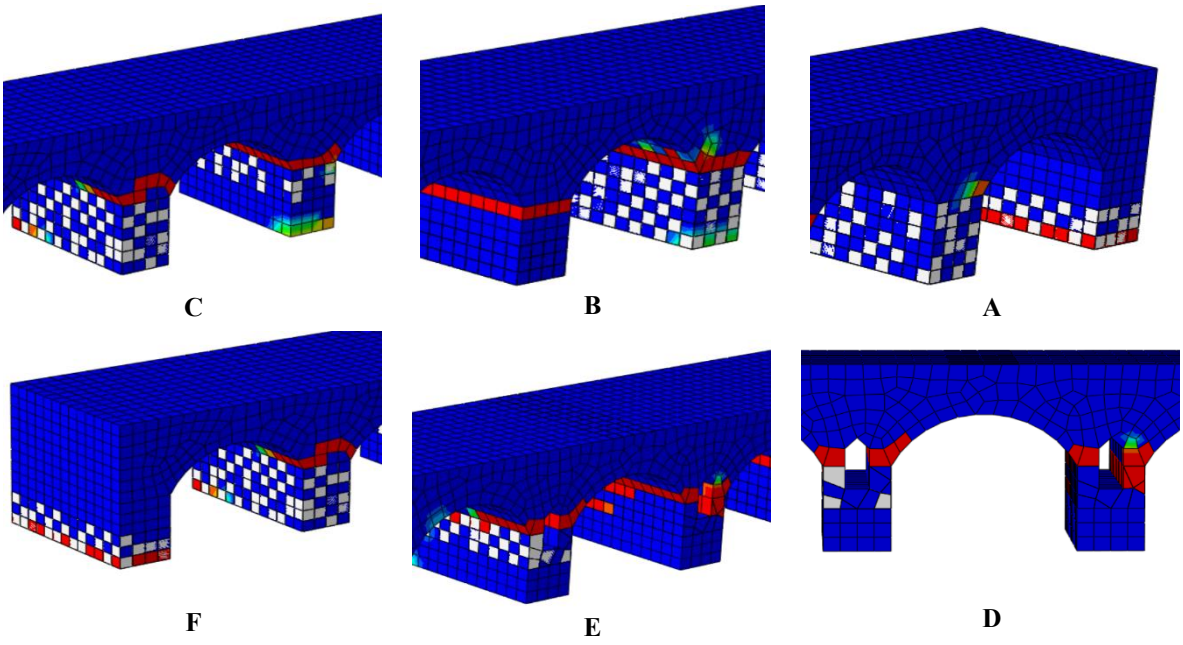

Fig. 24. The structural damage contour under the Manjil earthquake in the third retrofitting step.

but for the piers, given that with retrofitting each pier, the damage is transferred to another pier and finally reaches the point of attachment of the pier and the spandrel wall that this problem shows using these materials is not suitable for strengthening these sections, therefore, using this method is not suitable for the retrofitting of the piers.

4- 3- 2- Analyzing the results of the analysis in the three-component mode under the earthquake of Tabas and El Centro in a reinforced state

According to Figs. 25 to 28, the seismic performance of the studied bridge under the Tabas and El Centro earthquakes is almost the same as the Manjil earthquake. The retrofitting process under the two earthquakes is similar to the Manjil earthquake. In other words, by retrofitting a region of the piers, the damage is transferred to another area. So, retrofitting has been done step-by-step. To summarize, the results of retrofitting are presented in Figs. 25 to 28.

As shown in Fig. 25, the damage distribution range in the structure after the retrofitting, in addition to the piers, has also been expanded to the deck. In the following, the reinforced structure performance has been investigated under the El Centro earthquake.

The results of the analysis of the retrofitted structure under the El Centro earthquake (Fig. 26) reveal that the damage location on the deck, under this earthquake, has been transmitted to the lateral spans. In the following, the final step of bridge retrofitting under the Tabas and El Centro earthquakes has been studied.

The results of several retrofitting steps under the Tabas earthquake disclosed that FRP materials are not suitable for retrofitting the piers and even the deck because, according to Fig. 27, the damage of the deck have been expanded such as damage in the pier, and, unlike the Manjil earthquake damage does not remain in a constant region and is transferred from point to the point. Therefore, it can be concluded that the retrofitting of the studied bridge is not suitable under the Tabas earthquake by the FRP method and other methods should be used.

As shown in Fig. 28, until the final retrofit step under El Centro, no damage has occurred in the middle of the deck bridge, and the tensile cracks are mainly concentrated at both ends of the deck bridge. In addition, at the location of the openings in the piers, the shape of the cracks has changed and appeared vertically. The performance of the FRP-reinforced structure under the El Centro earthquake is such that the method studied is suitable for deck retrofit but is not cost-effective for retrofitting the piers like other earthquakes.

5- Conclusion

The Namroud masonry bridge was investigated under five earthquake records. All records are related to the near field with magnitudes greater than 6 Richter. At first, only the horizontal components of each earthquake were applied to the structure and the seismic response of the structure was investigated. The results indicated that the structure is not vulnerable to horizontal components of the earthquake. Then, in the second step, the vertical components of the earthquakes along with the horizontal components were also applied to the structure. After structural analysis, relatively moderate damage was observed under the Manjil, Tabas, and El Centro earthquakes, but under the Bam and Zarand earthquake, no

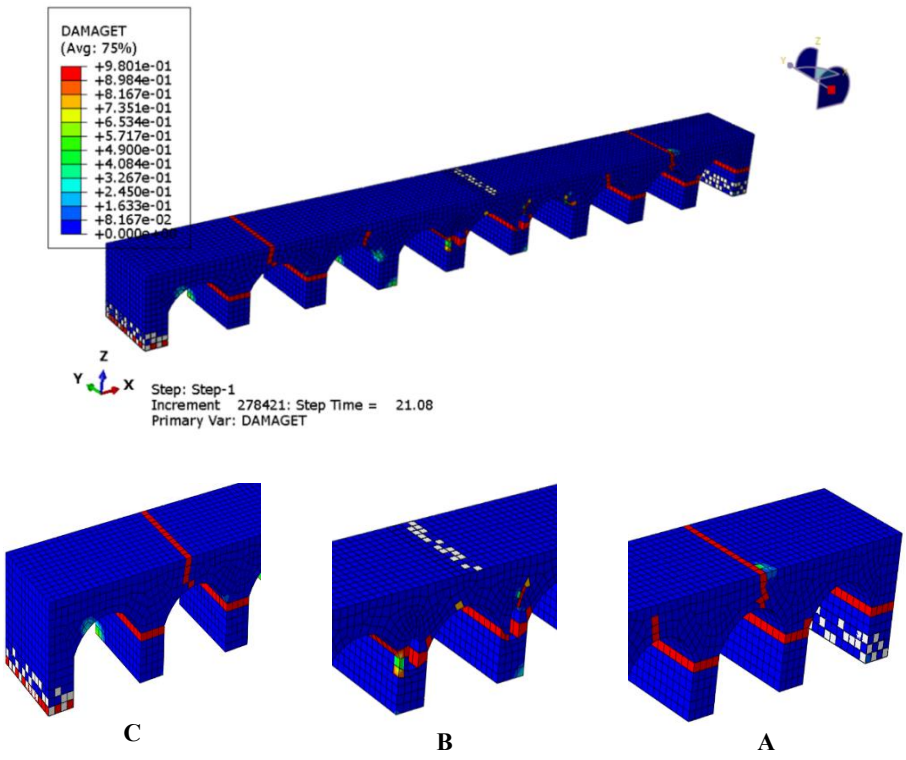

Fig. 25. The structural damage contour under the Tabas earthquake in the first step of retrofitting.

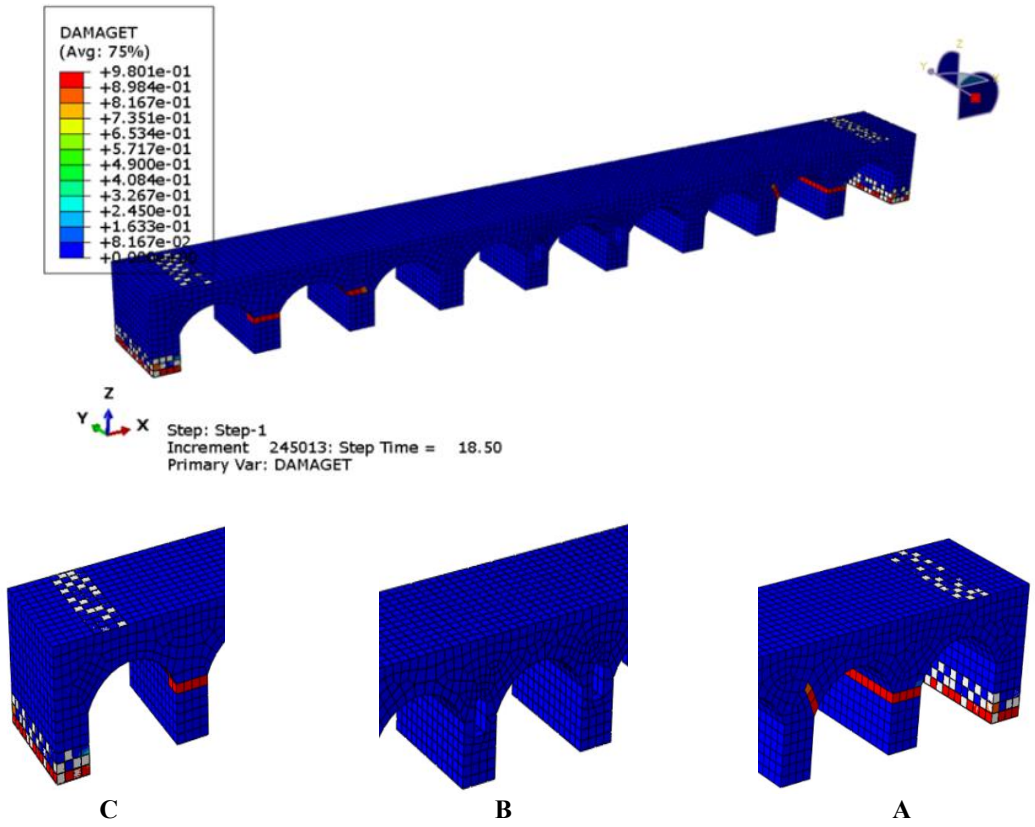

Fig. 26. The structural damage contour under the El Centro earthquake in the first step of retrofitting.

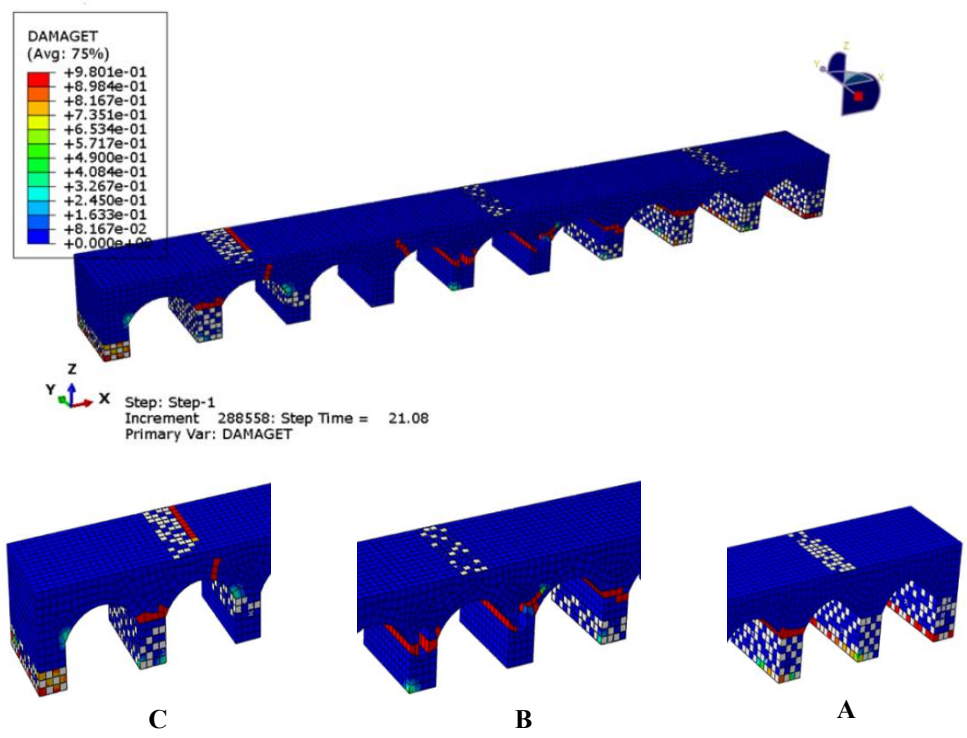

Fig. 27. The structural damage contour under the Tabas earthquake in the final steps of retrofitting.

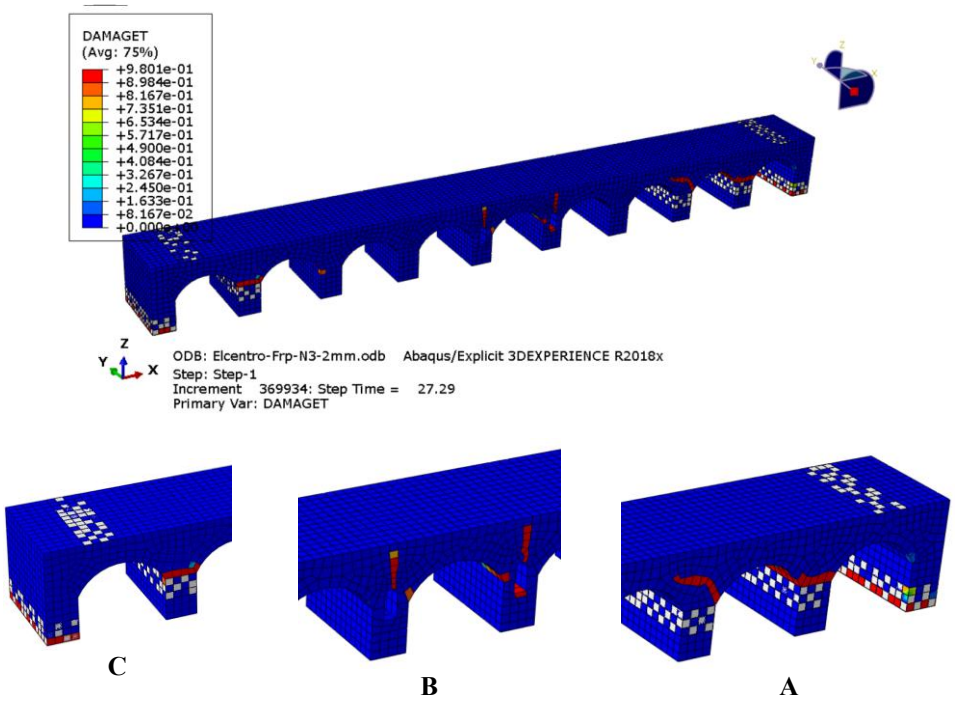

Fig. 28. The structural damage contour under the El Centro earthquake in the final steps of retrofitting.

significant damage occurred. The obtained results are as follows: the studied bridge, according to the standard of code 463, is vulnerable to earthquakes, but it can still maintain its sustainability. The vertical component has a significant impact on the vulnerability of the studied bridge, so the presence of the vertical acceleration component creates tensile cracks in the bridge piers and the deck. The studied retrofitting method, including the addition of FRP sheets to the outer surfaces of the bridge, was significantly effective in improving the seismic performance of the bridge in favor of reducing tensile cracks. The frequency content of earthquakes plays a vital role in the stimulation of the vibrational mode, the type, and shape of the damage, and finally the transfer of the cracks. Retrofitting by FRP in some parts of this structure leads to the spread of damage and transfer of damage from one area to another. In this bridge, the retrofitting of the deck by the FRP material was very efficient and the tensile tracks created were considerably reduced. In the location of the relatively small openings, due to the lack of access to all locations, there is no possibility of the desired performance of FRP materials; as a result, other methods of retrofitting should be used in these areas. At the location of the piers connection with the spandrel walls, FRP does not have good efficiency, and in these areas, other methods such as planting rebar, injection, etc. should be used. Generally, it is not possible to use just FRP material to achieve an economical and efficient method for retrofitting all parts of these types of bridges.

References

[1] J. Bień, T. Kamiński, Damages to masonry arch bridges, Wroclaw University of Technology, Institute of Civil Engineering, Wroclaw, Poland, 2007.

[2] T.E. Beuerman, Inventory of repairing and strengthening techniques for masonry arch bridges, Master's thesis, Universitat Politècnica de Catalunya, 2009.

[3] G. Frunzio, M. Monaco, A. Gesualdo, 3D FEM analysis of a Roman arch bridge, Historical constructions, (2001) 591-598.

[4] A. Özmen, E. Sayın, Seismic assessment of a historical masonry arch bridge, Journal of Structural Engineering, 1(2) (2018) 95-104.

[5] I.J. Drygala, J.M. Dulinska, Ł. Bednarz, J. Jasienko, Seismic performance of a masonry arch viaduct subjected to foreshocks and a mainshock, In MATEC Web of Conferences 211, 09003, EDP Sciences, 2018.

[6] D. Royles, A.W. Hendry, Model Tests of Masonry Arches. Proc. Inst. Civil Engineers Part 2, 1991.

[7] M. Begimgil, Behaviour of restrained 1.25 m span model masonry arch bridge, In First International Conference on Arch bridges, C. Melbourne, ed., Thomas Telford, Bolton, UK, 321-325, 1995.

[8] T.E. Boothby, D.E. Domalik, V.A. Dalal, Service load response of masonry arch bridges, Journal of structural engineering, 124(1) (1998) 17-23.

[9] P.J. Fanning, T.E. Boothby, Three-dimensional modeling and full-scale testing of stone arch bridges, Computers & Structures, 79(29-30) (2001) 2645-2662.

[10] A. Brencich, S. Donato, Experimental identification of a multi-span masonry bridge: The Tanaro Bridge, Construction and Building Materials, 22(10) (2008) 2087-2099.

[11] G. Milani, B.L. Paulo, 3D non-linear behavior of masonry arch bridges, Computers & Structures, 110 (2012) 133-150.

[12] B. Sevim, B. Alemdar, A. Ahmet Can, A. Sezer, B. Fatma, Finite element model calibration effects on the earthquake response of masonry arch bridges, Finite Elements in Analysis and Design, 47(7) (2011) 621-634.

[13] E. Sayın, Y. Calayır, M. Karaton, Nonlinear Seismic Analysis of Historical Uzunok Bridge, Seventh National Conference on Earthquake Engineering, 30 May–3 June, Istanbul, Turkey, 2011.

[14] L. Pelà, A. Alessandra, B. Andrea, Comparison of seismic assessment procedures for masonry arch bridges, Construction and Building Materials, 38 (2013) 381-394.

[15] E. Sayin, Nonlinear seismic response of a masonry arch bridge, Earthquakes and Structures, 10(2) (2016) 483-494.

[16] M. Karaton, H. S. Aksoy, E. Sayın, Y. Calayır, Nonlinear seismic performance of a 12th-century historical masonry bridge under different earthquake levels, Engineering Failure Analysis, 79 (2017) 408-421.

[17] M. Naderi, M. Zekavati, Assessment of seismic behavior stone bridge using a finite element method and discrete element method, Earthquakes and Structures, 14(4) (2018) 297-303.

[18] I.O. Demirel, A. Aldemir, Simplified Approach for Seismic Performance Assessment of Dry-Joint Masonry Arch Bridges, Buildings, 11(7) (2021), 313.

[19] R.W. Poole, I.W. Farmer, Consistency and repeatability of Schmidt hammer rebound data during field testing, International Journal of Rock Mechanics and Mining Science, 17(3) (1980) 167-171.

[20] T. Jankowiak, T. Lodygowski, Identification of parameters of concrete damage plasticity constitutive model, Foundations of civil and environmental engineering, 6(1) (2005) 53-69.

[21] Road and Railway Bridges Seismic Resistant Design Code; No: 463, Ministry of Roads and Transportation, Deputy of Training, Research and Information Technology, 2008.

HOW TO CITE THIS ARTICLE

M. MollaJafari, F. Emami , M. H. Hosseini, Seismic Performance Assessment of a Masonry Arch Bridge Using Finite Element Method and Retrofitting by FRP, AUT J. Civil Eng., 6(1) (2022) 63-82.

DOI: 10.22060/ajce.2022.20227.5764